ACI MATERIALS JOURNAL TECHNICAL PAPER

Title no. 84-M4

Statistical Extrapolation of Shrinkage Data—Part I: Regression

by Z. P. Bažant, F. H. Wittmann, J. K. Kim, and F. Alou

A large series of data on carefully controlled shrinkage tests of concrete involving groups of large numbers of identical specimens is reported. The data are used to compare existing shrinkage formulas in ACI, CEB-FIP, and BP models. By far the best agreement is obtained for the BP model. Assuming that only the measured data for a certain initial period are known, predictions are made for long times and are compared with the subsequently observed shrinkage strains. In this manner, various possible statistical regression models are examined and compared. Best predictions are obtained when the shrinkage formula is fitted to test data using nonlinear optimization, then linear regression in transformed variables is used to obtain the confidence limits for long-time predictions.

It is concluded that good long-time predictions of shrinkage can be obtained on the basis of shrinkage test results on 80 mm diameter cylinders for a 3-week duration. These predictions involve only the intrinsic uncertainty of the material, on which the uncertainty due to random environment, curing history, and differences in concrete composition must be superimposed for practical application.

Keywords: concretes; deformation; diffusion; drying; errors; **extrapolation; regression analysis; shrinkage;** statistical analysis; volume change.

Shrinkage, as well as creep, represents the most uncertain mechanical property of concrete, the statistical scatter of which considerably exceeds that of strength. Yet, in contrast to the design of structures for ultimate loads, the design for shrinkage is not currently based on statistical concepts. The aim of this paper is to establish the statistical properties of shrinkage that could be used in design. This is of interest especially for special structures sensitive to long-time deformations and cracking.

Prediction of shrinkage effects in structures can be made in two phases. The first phase, which is examined here, consists of determining the shrinkage properties of the material, and the second phase consists of the structural analysis based on these properties. The second phase, which inevitably involves the uncertainty of the method of structural analysis, is not covered here. The uncertainty involved in the first phase has five distinct sources:

1. The uncertainty due to the measurement error.
2. The uncertainty due to random variations of the environmental relative humidity and temperature.
3. The uncertainty due to the random variability of the material properties which results from the process of mixing, casting, and curing of concrete.
4. The uncertainty due to the random nature of shrinkage increments, which is a consequence of the stochastic nature of the microscopic physical mechanism of shrinkage.
5. The uncertainty of the shrinkage prediction model per se (i.e., the shrinkage formula), both its form and the values of its parameters.

The first source of uncertainty is not felt by the structure and should, therefore, be minimized by careful control of measurements. Proper smoothing of the results can also eliminate much of the random measurement error, although not its systematic part. The second source of uncertainty, which can be most effectively treated by spectral analysis of stochastic processes, has been the subject of other works[1-3] and will not be studied here. This type of uncertainty is important for real structures, but it is negligible for tests in a laboratory with good environmental control. Therefore, we strive to model only the third through fifth sources of uncertainty. These three sources together represent the material, or intrinsic, uncertainties, as opposed to the environmental influences which represent an external, or extrinsic, uncertainty.

The model uncertainty, due to the error of the shrinkage formula, is inevitable since without a mathematical model no statistical evaluation is possible. For the formulas used in the current codes, this uncertainty is huge. Statistics involving many thousands of data points from the literature have recently been reported,[4-6] and it has been found that the confidence limits that are exceeded by the errors with a 10 percent probability are about ± 86 percent of the predicted value for the current ACI 209 model,[7,8] and ± 118 percent for the current CEB-FIP Model Code.[9] For the re-

Received Sept. 3, 1985, and reviewed under Institute publication policies.

Z. P. Bažant, FACI, is a professor and director, Center for Concrete and Geomaterials, Northwestern University. Dr. Bažant is a registered structural engineer, serves as consultant to Argonne National Laboratory and several other firms, and is on editorial boards of five journals. He is Chairman of ACI Committee 446, Fracture Mechanics, and a member of ACI Committee 209, Creep and Shrinkage in Concrete; 348, Structural Safety; and joint ACI-ASCE Committee 334, Concrete Shell Design and Construction. He also serves as Chairman of RILEM Committee TC69 on creep, of ASCE-EMD Committee on Properties of Materials, and of IA-SMiRT Division H. His works on concrete and geomaterials, inelastic behavior, fracture and stability have been recognized by a RILEM medal, ASCE Huber Prize and T. Y. Lin Award, IR-100 Award, Guggenheim Fellowship, Ford Foundation Fellowship, and election as Fellow of American Academy of Mechanics.

ACI member F. H. Wittmann is a professor and director of the Laboratory for Building Materials, Swiss Federal Institute of Technology, Lausanne. He received the RILEM medal for his research on properties of hardened cement paste. He serves as chairman of RILEM TC 50-FMC, Fracture Mechanics of Concrete, and of RILEM TC 78-MCA, Model Code for Autoclaved Aerated Concrete. He is on the editorial board of several scientific journals. At present he is president of the International Association for Structural Mechanics in Reactor Technology and he holds the position of Honorary Advisory Professor at Tongji University, Shanghai, China.

ACI member J. K. Kim is an assistant professor in Civil Engineering at Korea Advanced Institute of Science and Technology. He obtained his BS and MS degrees from Seoul National University, and the PhD degree from Northwestern University. He is on the editorial board of the Journal of the Architectural Institute of Korea. *His research interests include inelastic behavior and fracture of concrete and reinforced concrete.*

F. Alou received his diploma in civil engineering at the Swiss Federal Institute of Technology, Lausanne. At present he is head of the concrete technology and materials testing section of the Laboratory for Building Materials, Swiss Federal Institute of Technology, Lausanne. For several years he directed special projects in civil engineering in Switzerland and in Brazil. His research activities are oriented towards the relation between the structure of concrete and creep and shrinkage.

cently established shrinkage formulas of the BP model,[4-6,10] which is better justified physically but is also more complicated, these confidence limits are found to be ±27 percent, which is still quite large.

From some limited examples it appears[6] that the uncertainty of shrinkage prediction can be drastically reduced if some short-time measurements of shrinkage of the particular concrete under consideration are made. The question of how to extrapolate such short-time data to obtain long-time shrinkage predictions and their standard deviations will be the principal goal of the analysis that follows.

Part II of this study will deal with the problem of how the long-time predictions can be improved by means of Bayesian reasoning. Another paper[11] examines the type of probability distributions of strains as well as strain increments, the correlation of short-time and long-time data, and the evolution of statistics with time.

STATISTICAL TEST DATA

Abundant as the test data on shrinkage in the literature may be, scant information exists on the statistical scatter of concrete of a certain given type. The test data in the literature[4,5] yield information on the statistical deviations of various concretes from the mean prediction formulas, but they do not suffice for extracting information on the statistical properties of one particular concrete considered apart from the uncertainties due to the randomness of environment and to the measurement errors. The only attempts to determine the statistical characteristics of one particular concrete seem to have been those of Alou and Wittmann,[12] and Reinhardt, Pat, and Wittmann.[13] A similar attempt for concrete creep has been made by Cornelissen.[14,15] More extensive data, however, are needed, and therefore a large series of measurements involving sizeable groups of identical specimens has been carried out at Swiss Federal Institute of Technology in Lausanne.

This test series, still in progress, involves 35 cylindrical specimens of diameter 160 mm (6.30 in.) and 36 cylindrical specimens of diameter 83 mm (3.27 in.). In addition, three cylindrical specimens of 300 mm (11.81 in.) diameter are also measured. The length of all cylinders is twice that of their diameter. The mean 28-day strength of standard concrete cylinders is f'_c = 33.2 MPa (4814 psi) and the modulus of elasticity (according to DIN 1045) at 28 days is 36.3 kN/mm² (5.26×10^6 psi). No admixtures, plasticizers, or air-entraining agents are used. The specific mass of concrete is 2418 kg/m³ (150.96 lb/ft³), and 1 m³ (31.31 ft³) contains 350 kg (158.76 lb) of cement, 168 kg (76.20 lb) of water, 608 kg (275.78 lb) of fine sand from 0 to 4 mm (0.1575 in.) size, 399 kg (180.98 lb) of coarse sand from 4 to 8 mm (0.1575 to 0.3150 in.) size, 399 kg (180.98 lb) of fine gravel from 8 to 16 mm (0.3150 to 0.6299 in.) size, and 494 kg (224.07 lb.) of coarse gravel from 16 to 31.5 mm (0.6299 to 1.240 in.) size. The corresponding volume fractions are 0.113, 0.168, 0.226, 0.148, 0.148, and 0.184, respectively, plus 0.013 for air. The cement (of type CPN from the plant at Eclepens near Lausanne) is approximately of ASTM Type I, with fineness defined by surface area 2900 m²/g (Blaine). All aggregate is from a glacial morraine, of rounded shapes. Mineralogically, all aggregate is composed of 40 to 46 percent calcite, 29 to 32 percent quartz, 8 to 13 percent residue of crystalline rocks of multimineral composition, predominantly quartzitic, and 12 to 18 percent of composite grains, essentially quartzitic.

Contrary to most previous shrinkage studies, it was decided to cure all specimens in a sealed state and keep them sealed until the instant of exposure to the drying environment. This is necessary to achieve a uniform state throughout the cross section of the specimen at the start of drying. When the specimens are cured in water, water diffuses into concrete, causing the moisture content to become higher near the surface than in the core. The accompanying nonuniform swelling produces significant residual stresses within the cross section prior to the start of drying. These stresses may even lead to microcracking. When these initial stresses are superimposed on the subsequent stresses due to drying shrinkage, a rather different pattern of microcracking results and different creep due to residual stresses is obtained, causing distortion of the shrinkage curve. This makes the theoretical evaluation of shrinkage tests of specimens cured in water difficult and ambiguous. Curing in a sealed state avoids these problems, and it also better simulates practical conditions

for most structures. To achieve sealed conditions, all specimens were kept in their molds until the very start of the shrinkage test. Commercially available impermeable molds, made of waxed-carton paper, have been used. The imperviousness of the molds has been checked by weighing regularly all specimens.

Deformations were measured by taking length readings between the ends of the specimens along the cylinder axis. Deformation gages with dials, provided by steel balls that fit into ring-shaped steel targets glued to the specimens, were used. In shrinkage tests, it is important to take the first length readings before the start of drying; therefore, the targets for deformation measurements were attached before the molds were stripped. Without this, a certain amount of initial shrinkage would have been missed, which has no doubt happened in many previous measurements. Alou[12] previously observed that appreciable shrinkage occurs already during the first minute after the start of drying exposure, even for the 16 cm diameter specimens.

All specimens were exposed to drying at the age of 7 days. The environmental humidity was 65 ± 5 percent, and the room temperature was 18 ± 1 C (64.4 ± 1.8 F) throughout the casting, curing, and shrinkage.

One reason for choosing different diameters was to explore the possibility of accelerated shrinkage testing on reduced-diameter specimens (the shrinkage halftime is approximately proportional to the square of diameter). To try an extreme case of acceleration, square prisms of 40 mm (1.575 in.) side are also being tested. Too small to be cast, these prisms were sawed from the 160-mm (6.30-in.) cylinders. It must be kept in mind that sawed specimens are not exactly similar to cast specimens, due to the so-called wall affect, the fact that in a mold-cast specimen there is always a surface layer which contains a smaller fraction of aggregate and a higher fraction of cement paste than the interior of the specimen. This layer alters shrinkage appreciably, as recently shown.[16]

The results of all measurements, and the means and standard deviations for the measured shrinkage strain values and their logarithms, are listed in Tables 1(a), (b), and (c) for D = 83, D = 160, and D = 300 mm (3.27, 6.30, and 11.81 in.), respectively.

First, it is of interest to note the dependence of the coefficient of variation on time and on the size of the specimen; see Fig. 1(a). We see that the coefficient of variation of the shrinkage strain first decreases with time and then stabilizes at a constant value of about 7 percent. This final stabilized value appears to be about the same for all the specimen sizes. Initially, however, for the smaller sized specimens the coefficient of variation is smaller. The aforementioned decrease of the coefficient of variation with time is due mainly to the increase of the mean value of shrinkage. The standard deviation of shrinkage strain shows the opposite tendency — it increases with time [Fig. 1(b)]. [The lines in Fig. 1(a) for the 300 mm (11.81 in.) diameter specimens represent extrapolations from the values observed for the smaller specimen sizes, since the number of specimens was too small to determine the statistics.] These results confirm earlier findings described in Reference 12.

SHRINKAGE FORMULA

In the most realistic approach, deterministic shrinkage should be described by differential equations in space and time, which reflect the nonuniform time-variable distributions of unrestrained shrinkage strain (and pore humidity) over the cross section of specimen or structural member, and take into account the residual stresses as well as the creep and cracking that they cause. This approach is the only one to link shrinkage deformation with its real physical mechanism.[17,18] The proper statistical generalization is then a Markov process or an additive stochastic process in time.[19] A considerable amount of research will be required before such a statistical approach becomes feasible in practice.

We will therefore characterize shrinkage by a closed-form algebraic formula representing the total mean shrinkage strain ϵ_{sh} in the cross section

$$\epsilon_{sh} = \epsilon_{\infty}\left[1 + \left(\frac{\tau_{sh}}{\hat{t}}\right)^{r}\right]^{-\frac{1}{2r}} \tag{1}$$

in which $\hat{t} = t - t_0$ = duration of drying, t = age of concrete, t_0 = age of concrete when drying started, and ϵ_{∞}, τ_{sh}, and r are material parameters which must be considered as random variables. For r = 1, Eq. (1) represents the formula used previously in the BP model.[4-6] ϵ_{∞} is the final shrinkage strain and τ_{sh} is called the shrinkage halftime. According to the BP model

$$\tau_{sh} = (\tau_0 D)^2 \tag{2}$$

where D = effective thickness of the cross section (double the volume-surface ratio), and $\tau_0 = a_s k_S / C_1$, $C_1 = C_1(t_0, T)$, $\epsilon_{\infty} = \epsilon_{sh_{\infty}}(1 - h^3)$, $\epsilon_{sh_{\infty}} = \epsilon_{s_{\infty}} f(t_0)$ in which C_1 = characteristic diffusivity of concrete, T = temperature, a_s = material parameter (statistical variables), k_S = shape factor indicated by diffusion theory, h = environmental relative humidity, $f(t_0)$ = function of age, and $\epsilon_{s_{\infty}}$ = material parameter (statistical variable). In our analysis t_0, h, T, C_1, and k_S will be fixed and the same for all specimens; there will be only three random material parameters: ϵ_{∞}, τ_{sh}, and r.

Many aspects of the foregoing formulas of the BP model have been justified physically:

1. That τ_{sh} is proportional to D^2 follows from the diffusion theory. This is well-known property of the linear diffusion theory; however, it has been shown that the same property applies for nonlinear diffusion theory with a humidity-dependent value of diffusivity [see Eq. (7.105) to (7.107) of Reference 18, pp. 232-233]. This fact is important because the diffusion equation for concrete is strongly nonlinear.[18]

2. Furthermore, as is shown in the Appendix, the diffusion theory also requires that, at the beginning of drying

Table 1(a) — Shrinkage strains (in 10^{-6}) measured for individual specimens and their statistics (D = 83 mm)

Specimen No.	Drying duration $\hat{t}$, days																		
	0.01	0.042	0.208	0.375	1	2	3	6	8	14	21	34	52	91	169	258	412	554	1105*
1	12	32	34	40	59	93	119	168	196	260	300	377	456	503	560	655	698	731	746
2	20	25	27	33	49	76	107	149	174	214	252	317	386	436	473	555	597	616	625
3	13	20	26	33	53	86	108	154	178	235	272	336	403	450	491	577	622	653	672
4	15	25	32	39	59	91	114	164	190	250	288	356	431	486	535	625	673	696	714
5	18	27	32	38	56	88	113	163	189	245	283	348	418	468	516	603	648	671	694
6	10	15	22	36	55	91	114	167	194	260	304	375	456	510	570	669	713	748	760
7	23	34	43	53	60	91	113	157	180	250	288	354	426	479	528	614	659	682	701
8	13	23	33	42	67	97	124	178	206	289	332	410	499	564	621	724	778	809	820
9	12	23	29	38	60	97	125	179	206	272	312	386	467	521	581	677	730	757	766
10	13	22	23	32	48	77	99	146	170	225	260	325	394	447	489	572	615	636	652
11	12	22	25	31	47	78	100	143	167	221	256	320	391	448	492	577	624	649	667
12	13	20	22	27	40	70	94	147	172	234	276	344	420	475	527	615	659	684	700
13	15	27	34	43	58	87	110	162	189	246	285	358	432	495	554	647	695	720	740
14	13	23	31	37	49	75	96	135	154	207	241	304	368	417	482	538	579	604	621
15	5	17	28	36	58	91	114	164	191	256	300	377	464	513	597	698	755	785	804
16	6	21	31	39	55	87	108	151	174	228	263	328	397	450	496	575	616	638	648
17	17	27	38	47	66	98	120	165	189	246	285	355	431	490	544	632	679	704	721
18	20	32	39	49	59	94	118	168	196	268	310	388	470	535	599	693	748	774	786
19	12	23	32	39	55	83	105	147	168	222	256	314	381	431	477	554	594	611	626
20	6	18	27	37	56	89	113	159	184	243	283	354	436	503	567	662	715	741	760
21	15	28	37	49	69	102	124	173	201	265	307	382	469	534	597	688	740	766	782
22	13	25	31	39	54	80	99	137	157	205	235	292	354	409	448	519	560	577	588
23	6	21	28	37	53	83	107	162	189	251	292	360	445	519	577	668	714	740	755
24	10	26	29	38	47	74	97	142	167	221	258	321	397	457	522	600	644	666	683
25	20	33	43	51	65	94	119	172	200	261	301	383	473	544	613	712	764	796	806
26	26	29	37	60	65	94	115	160	187	243	281	356	439	503	568	665	717	747	756
27	26	37	50	60	76	107	127	169	195	245	279	348	420	478	529	614	662	685	700
28	17	27	39	49	61	87	108	148	173	218	249	311	377	432	483	561	604	626	636
29	23	32	43	53	67	99	121	165	192	243	278	349	424	484	539	625	671	695	711
30	21	32	45	56	74	104	125	170	198	252	290	366	447	507	571	663	709	735	752
31	23	32	44	54	70	102	125	172	198	250	287	356	435	500	566	654	702	733	744
32	16	29	42	58	76	109	136	184	212	267	305	383	463	529	595	687	734	775	792
33	28	40	56	66	80	103	131	178	205	256	292	358	431	494	552	639	687	715	732
34	21	37	50	64	83	118	141	186	214	270	306	377	458	523	590	680	722	757	766
35	23	38	51	64	81	111	134	179	206	256	288	352	425	486	540	624	668	690	705
36	7	21	38	50	66	94	116	159	184	232	262	321	393	452	501	579	625	648	662
$\bar{\varepsilon}_{sh}$	16	27	35	45	61	92	115	162	187	245	282	351	427	485	541	629	676	702	716
s_{sh}	6.1	6.3	8.8	10.5	10.4	11.2	11.6	13.1	15.2	19.6	22.1	27.6	33.8	37.8	45.8	52.8	56.1	59.8	59.5
ω	39	24	25	24	17	12	10	8	8	8	8	8	8	8	8	8	8	9	8
$\bar{\varepsilon}^{L}_{sh}$	1.16	1.41	1.54	1.64	1.78	1.96	2.06	2.21	2.27	2.39	2.45	2.54	2.63	2.68	2.73	2.80	2.83	2.84	2.85
s^{L}_{sh}	0.194	0.104	0.107	0.101	0.074	0.053	0.044	0.036	0.036	0.035	0.034	0.035	0.035	0.034	0.037	0.037	0.037	0.038	0.037
ω^{L}	16.7	7.3	7.0	6.2	4.2	2.7	2.1	1.6	1.6	1.5	1.4	1.4	1.3	1.3	1.4	1.3	1.3	1.3	1.3

$\bar{\varepsilon}_{sh}$, s_{sh}, and ω = mean, standard deviation, and coefficient of variation (in percent) of the group of all specimens; $\bar{\varepsilon}^{L}_{sh}$, S^{L}_{sh}, and ω^{L} = mean of the logarithms of strains, their standard deviation and their coefficient of variation (in percent).

*Measured just before publication; not included in any calculations.

Table 1(b) — Shrinkage strains (in 10^{-6}) measured for individual specimens and their statistics (D = 160 mm)

Specimen No.	Drying duration $\hat{t}$, days																		
	0.01	0.042	0.146	0.313	0.94	2	3	6	8	14	21	34	52	91	169	258	412	554	1105*
1	10	21	26	32	47	62	76	107	123	164	190	243	298	369	445	537	611	657	667
2	6	15	21	28	45	59	71	102	115	227	176	225	276	343	410	489	564	601	609
3	5	15	20	23	27	42	55	85	100	141	168	221	277	350	425	515	590	639	653
4	5	21	27	38	51	65	75	100	114	148	172	217	253	328	393	469	538	571	580
5	11	21	27	37	48	65	77	108	124	165	194	246	301	371	450	539	614	663	678
6	6	22	32	43	64	83	97	130	147	190	222	273	333	410	490	588	662	714	721
7	4	12	17	23	31	49	64	97	114	157	186	238	295	361	432	521	598	643	667
8	7	16	23	29	39	54	65	93	109	148	173	222	274	345	420	507	588	624	635
9	4	20	29	37	50	66	80	111	130	174	206	258	320	398	478	572	658	701	708
10	15	34	47	56	65	88	104	140	158	203	233	287	347	424	505	594	668	718	727
11	2	10	15	18	21	37	51	80	96	134	159	206	234	317	403	488	565	604	618
12	13	25	33	34	37	56	66	98	118	162	194	251	310	393	474	572	654	704	716
13	15	29	38	47	58	76	83	114	132	172	198	254	307	390	461	564	638	682	681
14	2	12	20	29	42	58	69	96	113	152	179	232	285	359	435	519	593	635	642
15	6	17	22	27	40	53	65	96	113	154	183	235	293	370	454	548	628	676	685
16	11	16	20	25	33	48	58	85	100	141	169	219	270	343	417	501	572	617	625
17	7	12	18	27	40	54	64	89	104	141	168	217	331	344	418	502	575	620	630
18	10	23	27	29	36	53	65	99	116	158	189	243	306	387	472	566	648	701	708
19	4	9	16	21	27	43	53	78	94	129	153	200	249	320	390	472	544	582	589
20	10	36	45	51	60	78	89	119	135	174	201	250	303	375	450	534	609	647	656
21	4	10	18	26	32	47	58	87	104	147	178	232	289	370	452	548	625	673	683
22	12	29	37	48	56	81	97	134	152	197	227	279	339	417	496	586	660	706	718
23	9	18	25	33	42	59	69	97	113	151	180	229	284	360	441	532	615	659	673
24	11	20	26	37	50	64	78	109	127	165	194	244	292	365	437	521	594	637	657
25	6	22	31	47	62	76	91	123	138	180	209	260	315	392	472	561	637	682	702
26	7	21	27	36	48	60	75	107	131	163	194	247	301	379	458	551	631	679	691
27	5	12	20	27	38	47	58	85	102	137	164	212	263	333	409	499	575	616	624
28	11	27	39	48	56	70	85	113	129	163	186	235	285	356	430	517	589	636	648
29	5	12	17	25	36	56	76	114	134	179	212	270	326	409	491	582	658	720	738
30	10	20	23	29	42	51	65	92	107	145	172	222	272	344	423	511	588	638	646
31	10	18	22	31	40	50	64	93	110	148	174	225	278	352	429	576	587	632	646
32	12	26	34	42	53	64	80	111	127	165	192	240	292	365	442	532	613	652	658
33	13	25	33	44	58	67	81	107	123	158	184	232	281	354	431	517	590	636	651
34	4	16	23	33	45	58	72	102	120	159	186	239	293	370	450	538	614	655	661
35	4	13	17	27	37	45	59	86	102	137	162	208	258	330	408	492	568	610	616
$\bar{\varepsilon}_{sh}$	8	19	26	34	44	59	72	102	119	161	186	237	293	366	443	533	607	652	663
s_{sh}	3.7	6.7	8.2	9.4	11.2	12.5	13.1	15.0	15.7	20.9	19.0	20.8	25.5	27.1	29.5	34.1	34.9	38.9	39.4
ω	47	35	31	28	25	21	18	15	13	13	10	9	9	7	7	6	6	6	6
$\bar{\varepsilon}'_{sh}$	0.84	1.26	1.40	1.51	1.63	1.77	1.85	2.01	2.07	2.20	2.27	2.37	2.46	2.56	2.65	2.73	2.78	2.81	2.82
s'_{sh}	0.227	0.155	0.131	0.119	0.116	0.090	0.077	0.062	0.056	0.054	0.043	0.038	0.038	0.032	0.029	0.028	0.025	0.026	0.026
ω'	26.9	12.3	9.4	7.8	7.1	5.1	4.2	3.1	2.7	2.4	1.9	1.6	1.5	1.3	1.1	1.0	0.9	0.9	0.9

*Measured just before publication; not included in any calculations.

Table 1(c) — Shrinkage strains measured (in 10^{-6}) for individual specimens and their statistics (D = 300mm)

Specimen no.	t_1, days																
	0.104	0.229	0.89	2	3	6	8	14	21	34	52	91	169	258	412	554	1105*
1	18	22	31	40	45	58	65	82	107	131	160	200	278	347	436	498	562
2	18	24	31	38	42	56	65	85	102	131	156	196	276	338	396	436	522
3	18	22	29	38	38	53	60	80	105	125	151	196	269	336	403	461	520
$\bar{\epsilon}_{sh}$	18	23	30	39	42	56	63	82	105	129	156	197	274	340	412	465	535
$\bar{\epsilon}'_{sh}$	1.25	1.36	1.48	1.59	1.62	1.75	1.80	1.92	2.02	2.11	2.19	2.30	2.44	2.53	2.61	2.67	2.73

*Measured just before publication; not included in any calculations.

$$\text{for } \hat{t} << \tau_{sh}: \quad \epsilon_{sh} \approx \epsilon_0 (\hat{t}/\tau_{sh})^{1/2} \tag{3}$$

Indeed, Eq. (1) does asymptotically reduce to this form for very small $\hat{t}$. Note, however, that the formula $\epsilon_{sh} = \epsilon_\infty [1 + (\tau_{sh}/t)^p]_{-q}$ with arbitrary constants p and q would not satisfy this condition, and would, therefore, be inadmissible from the viewpoint of the diffusion theory (the applicability of which is verified by Fig. 2, considered later).

3. Diffusion theory also justifies coefficient k_s for the shape of the specimen, the effect of concrete permeability C_1 through τ_{sh}, and the effect of temperature through permeability C_1. Furthermore, the effects of temperature on τ_{sh} and on the equivalent age which influences ϵ_{sh_∞} result from the activation energy theory.

The aforementioned physical aspects of shrinkage are ignored by the formulas used in contemporary design codes [see Eq. (4) and (5)]. These code formulas are purely empirical.

For comparison we will also consider the formulas from the current recommendations of ACI and of CEB-FIP. The ACI recommendation[7,8] is

$$\epsilon_{sh} = \epsilon_\infty \frac{\hat{t}}{\tau_0 + \hat{t}} \tag{4}$$

in which ϵ_∞ and τ_0 are material constants specified in the recommendation. We consider ϵ_∞ and τ_0 as random variables.

The CEB-FIP Model Code[9] uses the expression

$$\epsilon_{sh} = \epsilon_\infty [\beta_s(t) - \beta_s(t_0)] \tag{5}$$

in which ϵ_∞ is a material parameter and $\beta_s(t)$ is a given function which is to be taken from graphs and is, therefore, difficult to randomize. Therefore, we consider only one random material parameter ϵ_∞.

REGRESSION

The random parameters are involved in our shrinkage formula [Eq. (1)] nonlinearly. Despite this nonlinearity, it is quite easy to obtain the mean parameter values which yield the optimal fit of the given test data with Eq. (1). The standard computer library subroutine for nonlinear optimization (according to the Marquardt-Levenberg algorithm) may be used for this purpose. Even though this algorithm also yields estimates of the standard deviations of the material parameters

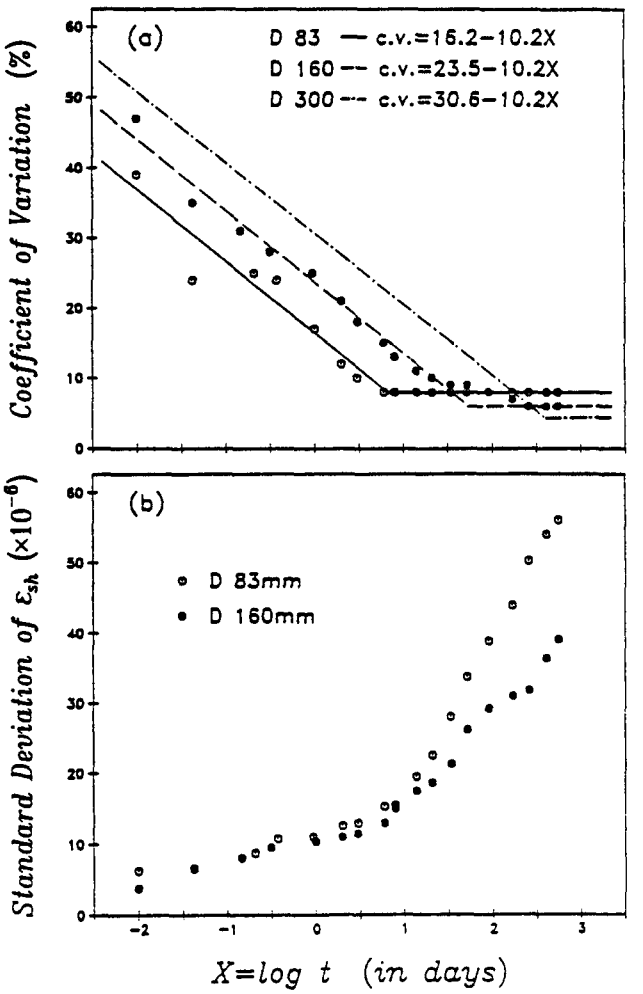

Fig. 1—Statistics of shrinkage strain as a function of time and specimen size

ϵ_∞, τ_{sh}, and r, it is clearer and more instructive to carry out the statistical analysis by regression. We will examine two types of regression.

Nonlinear regression

By using a standard computer library optimization subroutine which minimizes the sum of squared deviations from the formula, we first obtain the optimized mean values of the parameters of the shrinkage formula [Eq. (1), (4) or (5)]. In Eq. (1) we optimize only two parameters ϵ_∞ and τ_{sh} because the optimization for parameter r does not converge well and different values are obtained for various initial estimates (see Table 2).

Therefore, the value of exponent r is fixed in the optimization. Three possible values $r = 0.75$, 1, and 1.25 are tried, and the best one is identified at the end. The computer library subroutine also yields estimates of the standard deviations of all optimized parameters. These estimates are approximate, since they are obtained on the basis of a tangentially linearized regression model.

To predict the statistics of shrinkage strains at long times, we choose the sampling approach, for which the recently developed method of latin hypercube sampling[20-22] is most efficient. In this method, the practical application of which to a similar problem is developed in detail in Reference 23, the range of each parameter is subdivided into intervals of equal probability, based on an assumed distribution which is considered to be normal (Gaussian) for each parameter. If there are n intervals for each parameter, one chooses n latin hypercube samples of the parameters and calculates the shrinkage strain prediction for each sample. The sampling values of material parameter are chosen at the centroids of the aforementioned intervals, and a random selection of the sampled intervals is made under the restriction that each interval occurs in exactly one sample. Denoting the shrinkage strain predictions for various parameter samples as $\epsilon_{sh}^{(k)}$, with $k = 1,2, \ldots n$, the mean and the standard deviation of the prediction are

$$\bar{\epsilon}_{sh}(t_i) = \frac{1}{n} \sum_{k=1}^{n} \epsilon_{sh}^{(k)}(t_i),$$
$$s(t_i) = \left\{ \frac{1}{n} \sum_{k=1}^{n} \left[\epsilon_{sh}^{(k)}(t_i) - \bar{\epsilon}_{sh}(t_i) \right]^2 \right\}^{1/2} \quad (6)$$

in which t_i denotes the time for which the prediction is made. Assuming a normal distribution, an interval of any specified confidence can then be determined for each t_i.

The foregoing approach based on Eq. (1) has one shortcoming. The parameter samples taken from the extremes of the range may often be negative, both for ϵ_∞ and τ_{sh}. However, negative values are physically inadmissible; moreover they may yield a negative shrinkage value, which is also inadmissible, or may cause that the formula cannot be evaluated, e.g., when τ_{sh} has a negative value. A remedy may be obtained by changing Eq. (1) to the prediction of log ϵ_{sh} instead of ϵ_{sh}, and in-

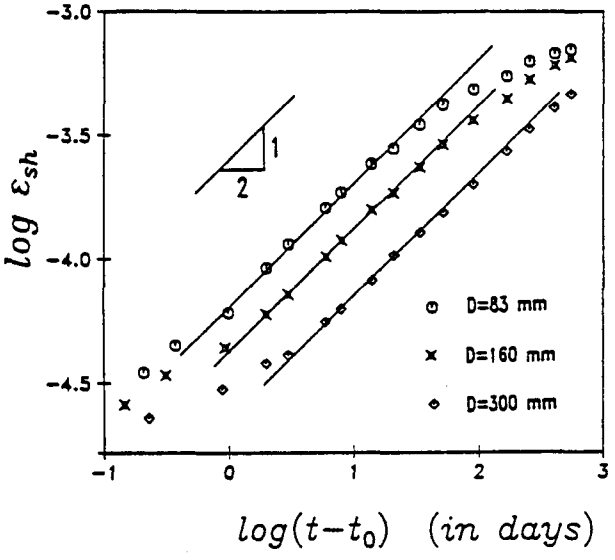

Fig. 2—Demonstration of agreement of mean of test results with slope one-half required by diffusion theory

Table 2 — Optimized mean values of random material parameters for Eq. (1), obtained by computer subroutine for Marquardt-Levenberg algorithm

D, mm	r	parameter ϵ_∞ (x10^{-6})	t_1, days: 21 mean	21 S.D.*	91 mean	91 S.D.	544 mean	544 S.D.
83	0.75	ϵ_∞	1093	235	963	51	866	12
		τ_{sh}	254	120	188	26	144	8
	1	ϵ_∞	711	107	752	25	772	10
		τ_{sh}	110	37	122	11	134	7
	1.25	ϵ_∞	556	63	656	16	728	11
		τ_{sh}	68	17	97	6	130	8
160	0.75	ϵ_∞	756	348	1215	175	1044	23
		τ_{sh}	298	292	788	254	566	37
	1	ϵ_∞	505	183	831	92	865	16
		τ_{sh}	133	108	380	95	423	25
	1.25	ϵ_∞	397	124	669	61	777	16
		τ_{sh}	-83	57	250	52	365	23
300	0.75	ϵ_∞	271	107	722	233	1475	150
		τ_{sh}	110	125	944	675	4316	999
	1	ϵ_∞	210	91	496	130	1019	82
		τ_{sh}	71	72	460	269	2123	392
	1.25	ϵ_∞	181	73	398	89	825	56
		τ_{sh}	55	51	303	151	1419	223

*S.D. = standard deviation.

Table 3 — Optimized mean values and standard deviations of random material parameters for Eq. (7), obtained by computer subroutine for Marquardt-Levenberg nonlinear optimization subroutine

D, mm	r	parameter	t_1, days: 3 mean	3 S.D.*	21 mean	21 S.D.	91 mean	91 S.D.	554 mean	554 S.D.
83	0.75	θ_1	-3.53	0.20	-3.04	0.17	-3.00	0.06	-3.05	0.02
		θ_2	1.20	0.14	2.24	0.36	2.31	0.13	2.20	0.05
	1	θ_1	-3.66	0.17	-3.21	0.14	-3.13	0.05	-3.12	0.02
		θ_2	0.95	0.39	1.91	0.30	2.06	0.11	2.09	0.04
	1.25	θ_1	-3.74	0.16	-3.30	0.12	-3.20	0.04	-3.15	0.02
		θ_2	0.81	0.36	1.73	0.26	1.94	0.10	2.04	0.04
160	0.75	θ_1	-4.03	0.06	-3.54	0.13	-3.21	0.13	-3.05	0.06
		θ_2	0.24	0.12	1.45	0.31	2.19	0.31	2.55	0.15
	1	θ_1	-4.10	0.06	-3.62	0.12	-3.31	0.12	-3.13	0.06
		θ_2	0.16	0.08	1.32	0.28	2.02	0.28	2.41	0.14
	1.25	θ_1	-4.13	0.06	-3.66	0.11	-3.36	0.12	-3.17	0.05
		θ_2	0.12	0.06	1.26	0.27	1.94	0.26	2.35	0.13
100	0.75	θ_1	-4.32	0.04	-3.95	0.10	-3.58	0.14	-3.14	0.14
		θ_2	-0.21	0.17	0.98	0.31	1.90	0.34	2.89	0.32
	1	θ_1	-4.36	0.04	-4.00	0.10	-3.64	0.13	-3.22	0.13
		θ_2	-0.19	0.16	0.93	0.28	1.81	0.31	2.73	0.29
	1.25	θ_1	-4.39	0.03	-4.03	0.09	-3.67	0.13	-3.27	0.12
		θ_2	-0.18	0.15	0.91	0.26	1.77	0.30	2.65	0.26

*S.D. = standard deviation.

troducing new parameters θ_1 and θ_2 which can take any real value, positive or negative. This is achieved by writing Eq. (1) in the form

$$\log \epsilon_{sh} = \theta_1 - \frac{1}{2r} \log \left[1 + \left(\frac{10_{\theta_2}}{t} \right)^r \right] \tag{7}$$

in which

$$\theta_1 = \log \epsilon_\infty, \quad \theta_2 = \log \tau_{sh} \tag{8}$$

This formula is equivalent to assuming that the distributions of ϵ_∞, τ_{sh}, and ϵ_{sh} are lognormal instead of normal. Eq. (7) means that the errors of shrinkage strain are multiplicative (relative) rather than additive, i.e., $\epsilon_{sh} = \bar{\epsilon}_{sh}(1 + \psi)$ rather than $= \bar{\epsilon}_{sh} + \psi$, in which ψ is a normally distributed random variable of zero mean and $\bar{\epsilon}_{sh}$ is a deterministic value (mean shrinkage).

Based on this approach [Eq. (7) and (8)], the optimized (mean) parameter values and their standard deviations have been obtained (see Table 3).

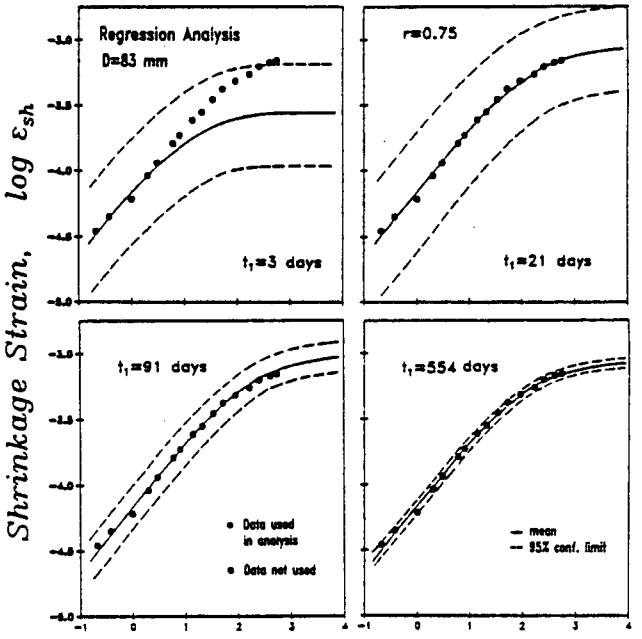

Fig. 3(a)

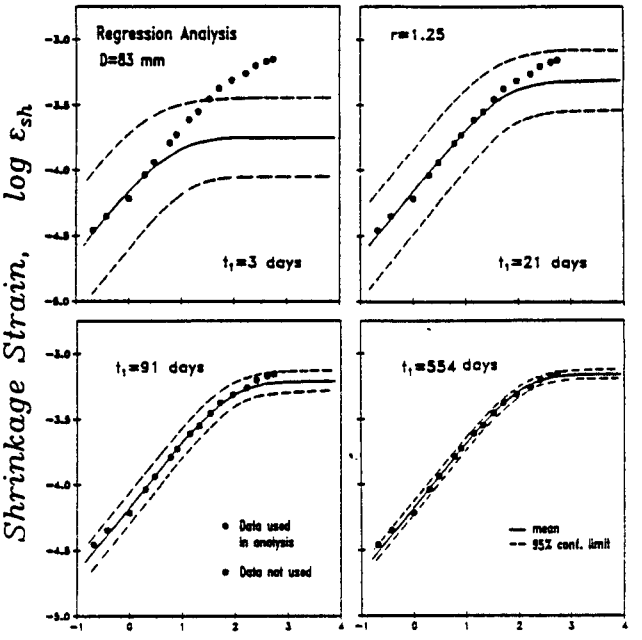

Fig. 3(c)

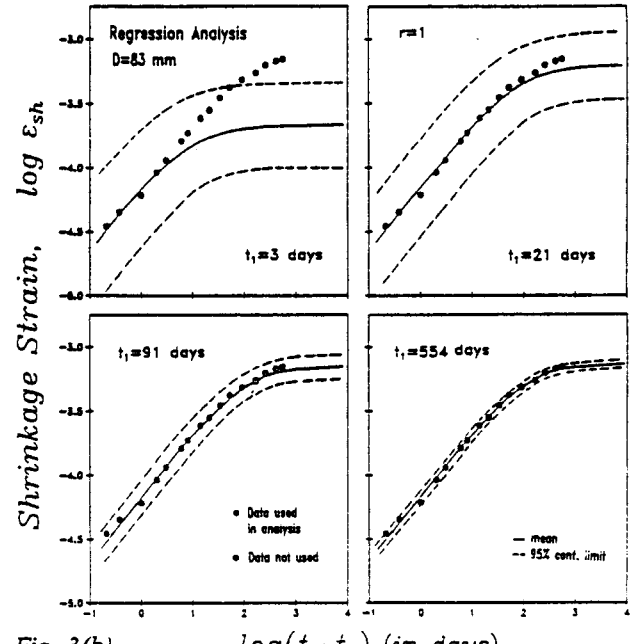

Fig. 3(b)

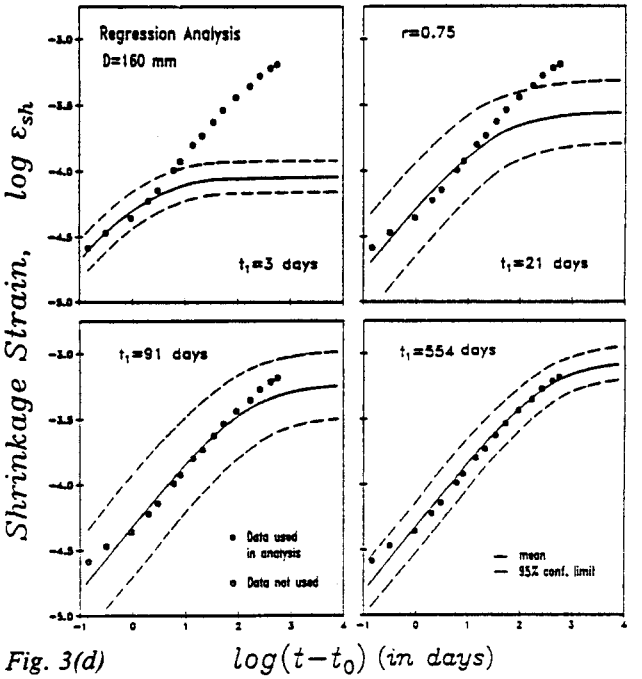

Fig. 3(d)

Fig. 3(a) through (f)—Means and 95-percent confidence limits predicted on the basis of data up to time t_1 *(solid points), compared to subsequently measured data (empty points). Calculated from standard deviations of random material parameters*

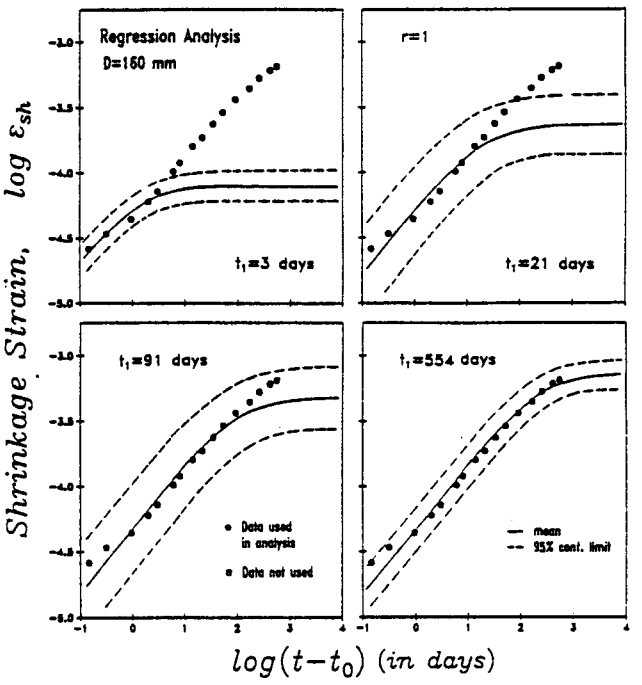

Fig. 3(e)

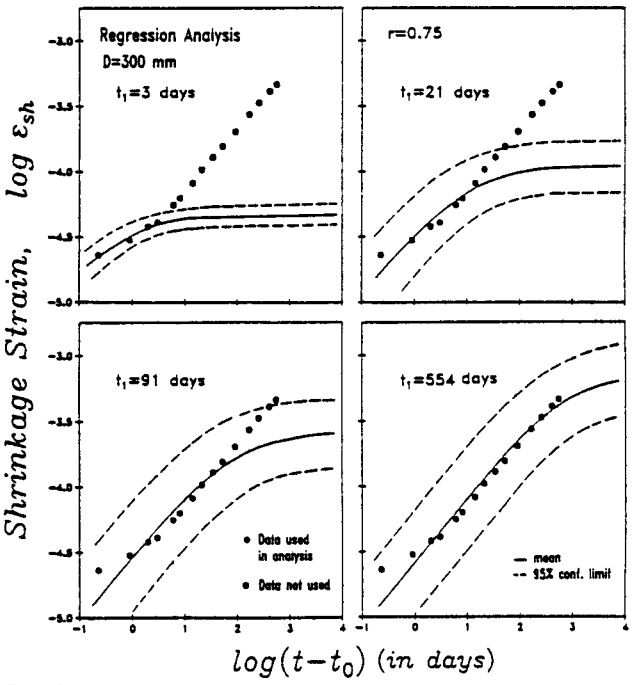

Fig. 3(g)

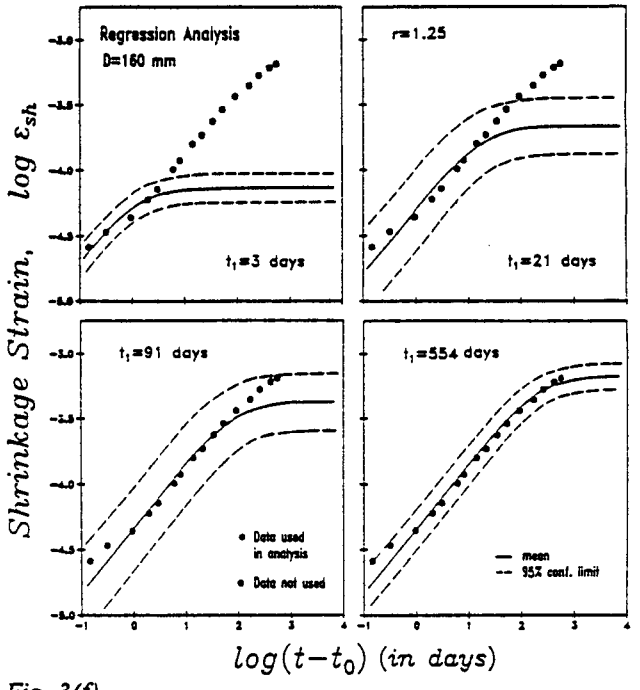

Fig. 3(f)

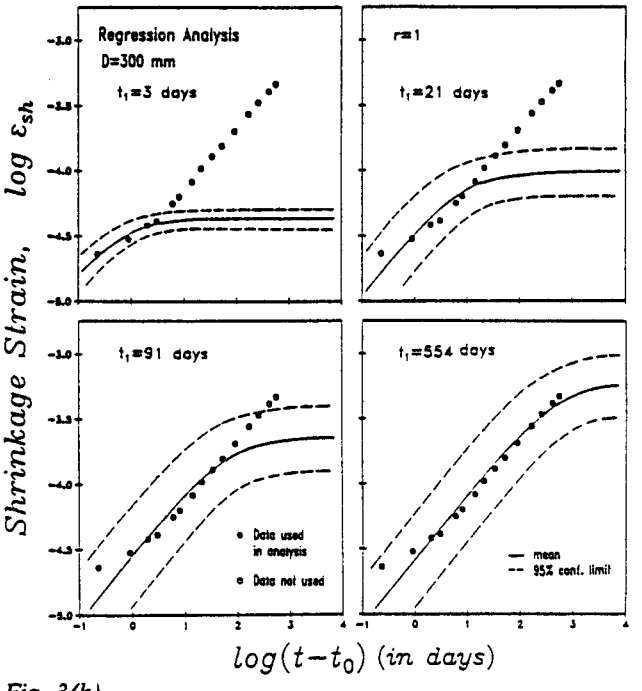

Fig. 3(h)

The predictions obtained in this manner are plotted in Fig. 3(a) through (i). In these figures the solid curves represent the means, and the dashed curves represent the 95 percent confidence limits (i.e., the limits that are exceeded with the probability of 2.5 percent on the plus side and 2.5 percent on the minus side). The predictions are plotted for various specimen sizes and for various chosen values of exponent r.

To assess the quality of the predictions, we now assume that the measured data are known only up to a certain chosen time t_1, as indicated in the figures by the solid data points, and that the subsequent measurements, shown as the empty data points, are unknown to us (Fig. 3). Obtaining the long-time prediction based only on the solid data points and comparing it with the subsequently measured (empty) data points we can see how good the prediction is. As expected, the longer the time span of measured data, the better the subsequent prediction (Fig. 3). Among various values of r, the best results are obtained with $r = 0.75$. To obtain good prediction for the specimens of 83 mm (3.27 in.) diameter, it suffices that the measured data be given up to the time $t_1 = 21$ days. For the specimens of 160 mm (6.30 in.) diameter, a much longer period of measurement is required to obtain a good prediction. Based on the size-square scaling of diffusion, one might expect

that $t_1 = 4 \times 21$ days = 84 days would be sufficient. However, as is apparent from Fig. 3(d) through (f) measurements of a duration longer than 91 days are required for the specimens of 160 mm diameter.

Aside from statistical predictions, the measured diagrams confirm that the trend of shrinkage based on diffusion theory, which requires the initial shrinkage curve to be described by Eq. (3), is correct (Fig. 2). According to this equation, the shrinkage curve in a log-log plot should be initially a straight line of slope exactly 0.5. All test data agree with this slope extremely well, except for some small deviation during the first few hours of shrinkage (for D = 83 mm) or the first day of shrinkage (for D = 160 mm). This deviation is probably due to the fact that the surface humidity of the cylinder does not become equal to the environmental humidity instantly, as assumed in the determination of the exponent ½ (see Appendix I), but with a delay due to a finite, rather than infinite, value of the moisture transmission coefficient at the surface. The shrinkage curves for the three specimen sizes are plotted together in Fig. 2, again making the straight-line slope of ½ conspicuous.

Finally, the shrinkage prediction according to Eq. (1) (BP model) is compared in Fig. 4 with those according to ACI and CEB-FIP [Eq. (4) and (5)]. In this comparison, the advantage of using a formula based on the diffusion theory is particularly striking. The curves in Fig. 4 are plotted exactly according to material parameter values from each prediction model, i.e., no attempt to fit the data is made. It is certainly by luck that the BP model prediction in Fig. 4 agrees with the measured data almost exactly; the overall accuracy of the BP model is not as good as that in Fig. 4. Note that even if the parameters of the ACI and CEB-FIP models were adjusted the initial slopes cannot be changed.

Combined nonlinear and linearized regression

Eq. (1) can be algebraically transformed to the linear equation

$$Y = AX + C \qquad (9)$$

in which

$$X = \frac{1}{t^r}, \quad Y = \frac{1}{\epsilon_{sh}^{2r}}, \quad A = \left(\frac{\tau_{sh}}{\epsilon_\infty^2}\right)^r, \quad C = \frac{1}{\epsilon_\infty^{2r}} \qquad (10)$$

This means that the plot of Y versus X should ideally be a straight line of slope A and Y-intercept C.

Simple though the straight-line regression according to Eq. (9) might seem, problems are encountered in practice. Due to random errors, the regression line of the measured data points plotted as Y versus X may yield a negative value of Y-intercept C, which is physically inadmissible. Furthermore, linear regression implies the statistical model $Y = AX + C + e$ in which e = error = normally distributed stochastic variable of zero mean, but an error e which appears small in the linear regression plot may translate, due to the transformations in Eq. (10), into a very large error in ϵ_{sh} if the shrinkage duration is very large. This causes that a

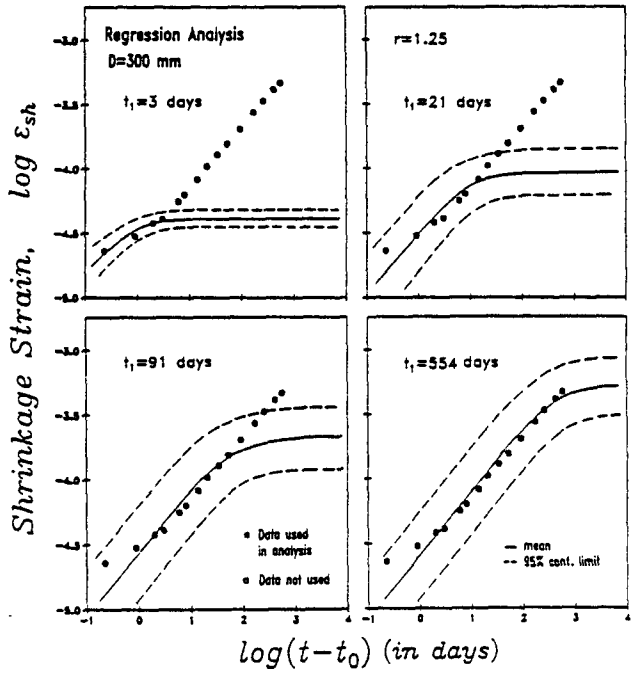

Fig. 3(i)

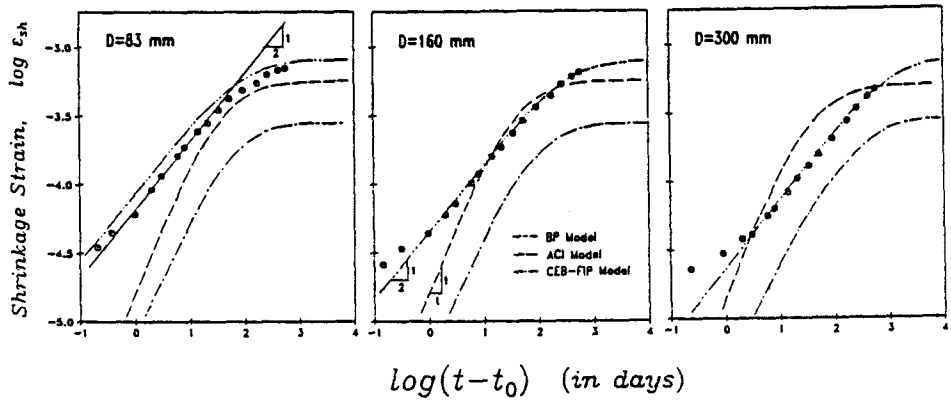

Fig. 4—Comparison of various models in the log-log plot (initial slope should be one-half, according to diffusion theory)

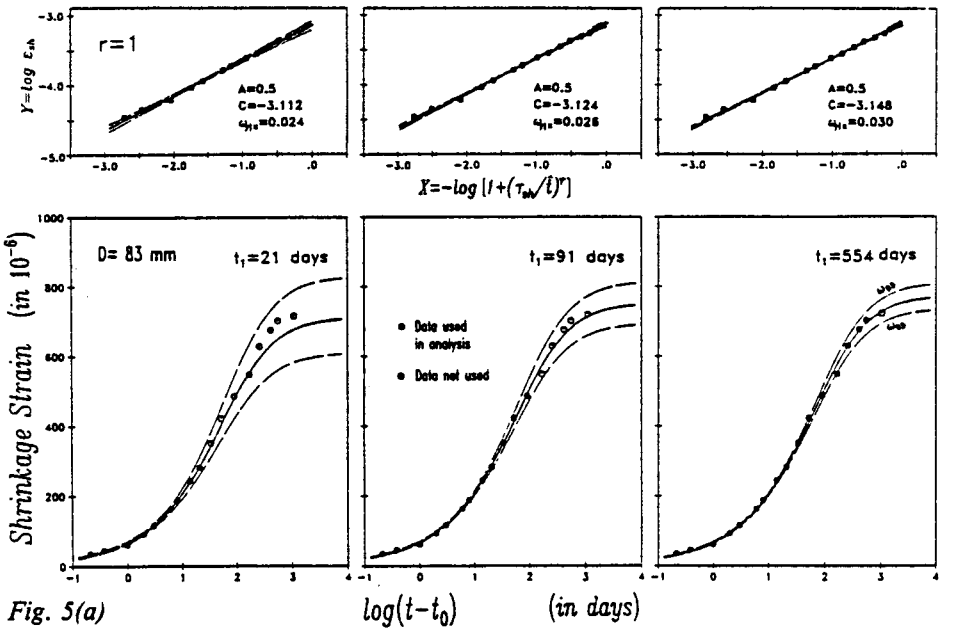

Fig. 5(a)

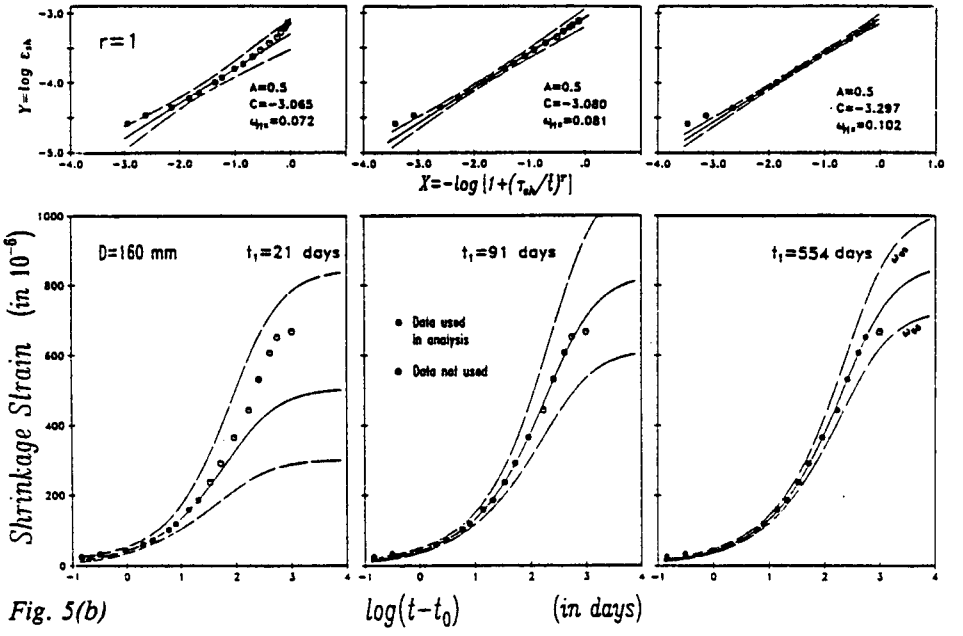

Fig. 5(b)

Fig. 5(a) through (c)—Means and 95-percent confidence limits predicted on the basis of data measured up to time t_1 *(solid points), compared to subsequently measured data (empty points). Calculated by a combination of nonlinear optimization and linear regression (last readings at 1105 days not included in any calculations)*

straight regression line is not sufficiently sensitive to the statistical scatter for short times and is oversensitive to the statistical scatter for long times. In consequence of this, it appears more realistic to measure the errors in terms of ϵ_{sh} than in terms of $Y = \epsilon_{sh}^{-2r}$, but then nonlinear optimization is required.

Another linear transformation leads to a regression equation [Eq.(9)] in which the additive error e is more reasonable

$$X = -\log\left[1 + \left(\frac{\tau_{sh}}{\hat{t}}\right)^r\right], \qquad (11)$$

$$Y = \log \epsilon_{sh}, \quad A = \frac{1}{2r}, \quad C = \log \epsilon_\infty$$

However, this has the disadvantage that the regression does not determine the shrinkage half-time τ_{sh}, an important parameter, while it determines, from the slope of the regression line, the value of exponent r to which the shrinkage predictions are quite insensitive except near the final shrinkage value. Therefore, it appears unsuitable to determine the material properties by linear regression.

In general, the straight-line regression plot of Y versus X has the fault that a good fit in the linear regression plot does not correspond to a good fit in the plot of ϵ_{sh} versus $\log \hat{t}$. For this reason, the material parameters should be determined by nonlinear optimization. Linear regression, however, still remains the sim-

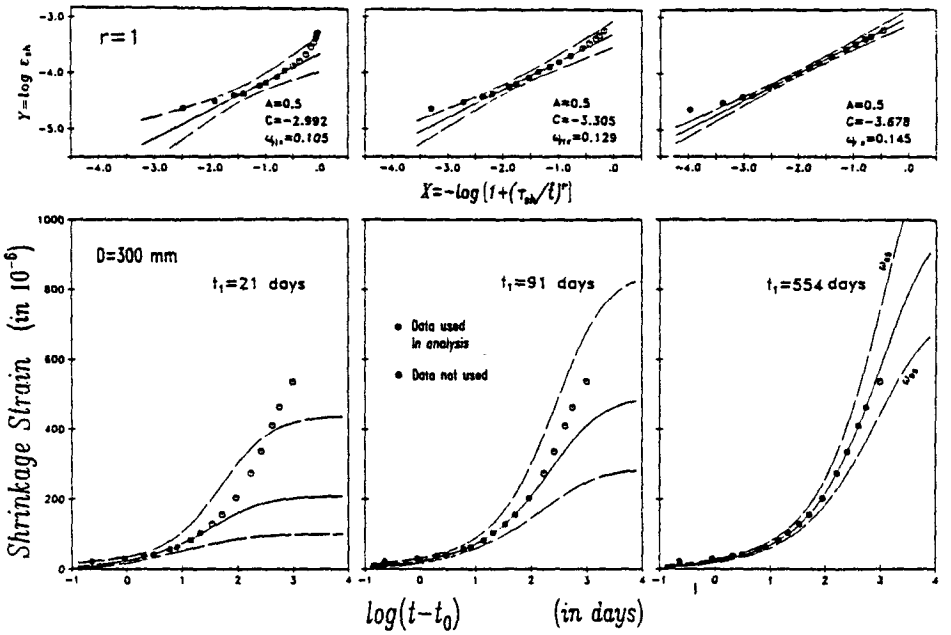

Fig. 5(c)

plest and most effective tool for handling the statistics of errors. Therefore, the following hybrid prediction procedure is adopted:

1. The optimum values of material parameters ϵ_{∞}, τ_{sh}, and r are obtained by a computer library subroutine for nonlinear optimization, as in the previous method. However, the confidence limits for the material parameters are not determined during this optimization. (As explained before, the value of r is fixed during this optimization; the optimization is repeated for various r-values and the one which gives the best result is selected at the end.)

2. Subsequently, linear regression formulas are used to determine the coefficient of variation $\omega_{y|x}$ for the vertical deviations from the straight regression line. From this, the confidence limits on log ϵ_{sh} are determined from the usual formulas for linear regression.

Application of this regression method to the present shrinkage data is shown in Fig. 5(a) through (c) for all three specimen sizes. In this type of regression, the results for $r = 1$ are no worse than those for any other r value; therefore $r = 1$ is used, which corresponds to the original BP model. The data points in Fig. 5(a) through (c) [as well as those in Fig. 3(a) through (i)] represent the mean value for each group of specimens — 36 specimens of diameter 83 mm (3.27 in.) 35 specimens of diameter 160 mm (6.30 in.) and 3 specimens of 300 mm (11.81 in.) diameter. The coefficient of variation $\omega_{y|x}$ pertains to the variability of these means, not of the individual specimen strains. Thus, the predicted long-time shrinkage and confidence limits pertain to the mean values of each group, not to the individual specimen strains.

The straight-line regression plots with 95 percent confidence limits are shown on top of each figure, and at the bottom of each figure the same mean curves and 95 percent confidence limits are shown in the plot of ϵ_{sh} versus the logarithm of drying duration $\hat{t} = t - t_0$ (Fig. 5). Note that the very small spread of the confidence limits on both ends of the linear regression plot corresponds, in the plot of ϵ_{sh} versus log $\hat{t}$, to a very narrow spread of confidence limits at very short times and a much broader spread of these limits at very long times.

To check how good the regression model is, the regression analysis is again carried out assuming that only the data points up to time t_1, shown as solid points, are known. The predictions may then be compared with the subsequently measured data points, which were not used in the analysis and are shown as empty points. The predictions are very good for the 83-mm (3.27-in.) and 160-mm (6.30-in.) specimens when t_1 = 91 days, and acceptable when t_1 = 21 days. For the 300 mm (11.81 in.) specimens (for which the coefficient of variations ω has been assumed rather than determined from the data), the prediction is poorer, but acceptable when t_1 = 91 days. For t_1 = 21 days, the prediction is still very good for the 83-mm specimens, and even t_1 = 3 days yields, for this specimen size, a practically sufficient accuracy of prediction.

Note how in Fig. 5(a) through (c) the confidence limits are getting wider with extrapolation into the future, and narrower as the duration of the data used for prediction increases. Furthermore, Fig. 6 illustrates that the proportionality of τ_{sh} with D^2 agrees with our data reasonably well. This means that the effects such as aging and heating due to hydration, which in theory should spoil the size-square dependence because they are stronger in larger specimens, were not important, although noticeable.

In the comparison of our two regression methods, the second, i.e., the combined nonlinear-linear regression, appears to yield better long-time predictions.

From the foregoing considerations it is clear that, on a strictly theoretical basis, it is difficult to make a choice between various possible regression models. This choice must be based on experience with making pre-

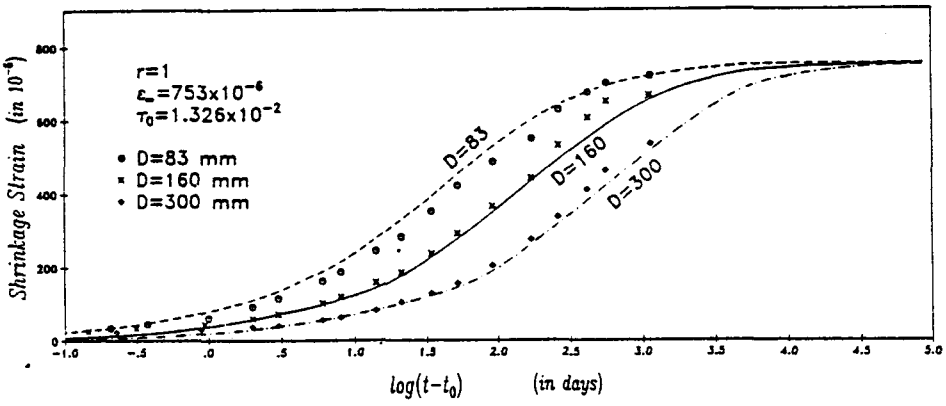

Fig. 6—Fit of measured data for various specimen sizes using a common value of τ_0 (last points at 1105 days were not included in fitting)

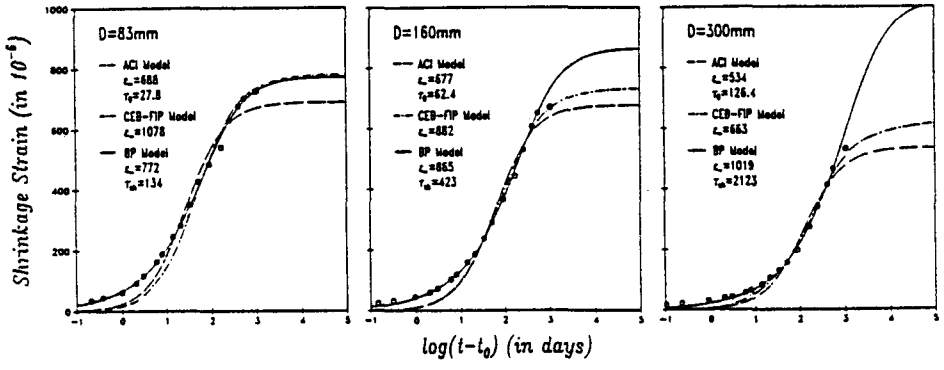

Fig. 7—Optimum fit of mean test data for various formulas in log time (last points at 1105 days not included in fitting)

dictions and comparing them with subsequent measurements. During the progress of the present measurements, predictions of future shrinkage strains were made at various stages before the outcome became known. For these predictions, the computer library nonlinear optimization subroutine with estimates of the standard deviations of material parameters was used, followed by latin hypercube sampling of the parameter values. This was done, however, in the plot of log ϵ_{sh} versus log t, rather than in the plot of ϵ_{sh} versus log t. The predictions which were obtained in this manner are shown in Fig. 3(a) through (i) where they may be compared with the subsequently measured data points (empty points) not known at the time of prediction. These predictions made during the progress of measurements were worse than those we are able to construct after all measurements are done. However, knowledge of the complete data is necessary to identify the best statistical regression method among the numerous possibilities that exist. Presumably, having decided this question, we would now be able to make better long-time predictions during the progress of measurements if this study were to be repeated.

So far we have been preoccupied with statistical extrapolation of short-time data. Another extrapolation of interest is that from small to large sizes. The present shrinkage measurements make it possible to check the size effect in the BP-model. To this end, we use the computer-library nonlinear optimization subroutine to fit the data for all specimens simultaneously, using Eq. (1) and (2) with ϵ_∞, τ_0 (rather than ϵ_∞, τ_{sh}) as the unknown parameters (r is fixed as 1). The resulting optimal fit is compared to all measured shrinkage data in Fig. 6. As we see, the agreement is reasonable. The deviations are probably due to the effects of aging and microcracking, and in the largest specimens probably also to hydration heat. The best possible fits according to the ACI, CEB-FIP, and BP formulas are also shown in Fig. 7. The agreement of ACI and CEB-FIP formulas with the data is worse than for the BP model.

CONCLUSIONS

1. The present shrinkage measurements, which appear to represent by far the largest statistical set of data obtained so far, show that the statistical scatter due to the intrinsic material uncertainty of shrinkage of concrete cast from one batch is rather small, with standard deviation of only about 7 percent of the mean shrinkage strain. Thus, the very large uncertainty of shrinkage in design as practically experienced is due mainly to the unknown and uncertain effects of concrete composition, along with its curing history, and to the randomness of environment.

2. Among ACI, CEB-FIB, and BP models, the latter one appears by far the best, and is also physically better justified.

3. As a basic simple consequence of diffusion theory, the plot of the logarithm of shrinkage strain versus the logarithm of drying duration should initially have a slope of ½. This property, which is exhibited by the BP model and is essential for making extrapolation of short-time data possible, is verified experimentally with great precision. The ACI and CEB-FIB models blatantly disagree with this property.

4. Although the shrinkage formula of the BP model can be linearized, statistical prediction of long-time shrinkage based on the linearized regression plot alone does not yield the best results. The best results are obtained by a combination of nonlinear least-square optimization for determining the mean values of material parameters and a linearized regression for determining the coefficients of variation.

5. The present data agree reasonably well with the size-square dependence of the shrinkage half-time (Fig. 6), indicated by diffusion theory and used in the BP model.

6. Specimens of reduced size may be used as a means of accelerated testing of shrinkage. Long-time shrinkage can be predicted well on the basis of three- or four-week measurements of shrinkage of cylinders with diameter 80 mm (3.15 in.).

7. By carrying out short-time (3-week) accelerated shrinkage tests for the given concrete to be used in a particular structure, one eliminates most of the shrinkage uncertainty due to concrete composition, which is the largest source of error. However, the statistical variation due to random environment, which is very large, must be superimposed on the long-time predictions obtained with the method proposed here.

8. The prediction based on minimizing the sum of squared errors in ϵ_{sh} is better than the prediction based on minimizing the sum of squared errors in $1/\epsilon_{sh}^2$. Whereas the latter prediction can be obtained by linear regression in transformed variables, the former prediction necessitates the use of a nonlinear optimization subroutine, such as the Marquardt-Levenberg algorithm.

ACKNOWLEDGMENT

Partial financial support obtained from the U.S. National Science Foundation (under grant No. FED 7400 to Northwestern University) and from the Swiss Federal Institute of Technology is gratefully appreciated.

REFERENCES

1. Bažant, Z. P., "Response of Aging Linear Systems to Ergodic Random Input," *Journal of Engineering Mechanics,* ASCE, V. 112, No. 3, Mar. 1986, pp. 322-342.

2. Bažant, Zdeněk P., and Wang, Tong-Sheng, "Spectral Analysis of Random Shrinkage Stresses in Concrete," *Journal of Engineering Mechanics,* ASCE, V. 110, No. 2, Feb. 1984, pp. 173-186.

3. Bažant, Zdeněk P., and Wang, Tong-Sheng, "Spectral Finite Element Analysis of Random Shrinkage in Concrete," *Journal of Structural Engineering,* ASCE, V. 110, No. 9, Sept. 1984, p. 2196-2211.

4. Bažant, Z. P., and Panula, L., "Practical Prediction of Time-Dependent Deformations of Concrete," *Materials and Structures, Research and Testing* (RILEM, Paris), V. 11, No. 65, Sept.-Oct. 1978, pp. 307-328; V. 11, No. 66, Nov.-Dec. 1978, pp. 415-434; and V. 12, No. 69, May-June 1979, pp. 169-183.

5. Bažant, Zdeněk P., and Panula, Liisa, "Creep and Shrinkage Characterization for Analyzing Prestressed Concrete Structures," *Journal,* Prestressed Concrete Institute, V. 25, No. 3, May-June 1980, pp. 86-122.

6. Bažant, Zdeněk P., and Panula, Liisa, "New Model for Practical Prediction of Creep and Shrinkage," *Designing for Creep and Shrinkage in Concrete Structures,* SP-76, American Concrete Institute, Detroit, 1982, pp. 7-23.

7. ACI Committee 209, "Prediction of Creep, Shrinkage, and Temperature Effects in Concrete Structures," *Designing for Effects of Creep, Shrinkage, and Temperature in Concrete Structures,* SP-27, American Concrete Institute, Detroit, 1971, pp. 51-93.

8. ACI Committee 209, "Prediction of Creep, Shrinkage, and Temperature Effects in Concrete Structures," (ACI 209R-82), American Concrete Institute, Detroit, 1982, 108 pp.

9. *CEB-FIP Code for Concrete Structures,* 3rd Edition, Comité Euro-International du Béton/Fédération Internationale de la Précontrainte, Paris, 1978, 348 pp.

10. Bažant, Zdeněk P., and Zebich, Steven, "Statistical Linear Regression Analysis of Prediction Models for Creep and Shrinkage," *Cement and Concrete Research,* V. 13, No. 6, Nov. 1983, pp. 869-876.

11. Bažant, Z. P.; Wittmann, F. H.; Kim, J. K.; and Alou, F., "Statistics of Shrinkage Test Data," *Report* No. 86-6/694s, Center for Concrete and Geomaterials, Northwestern University, Evanston, June 1986, 26 pp.

12. Alou, F., and Wittmann, F. H., "Etude expérimentale de la variabilité du retrait du béton," *Proceedings,* International Symposium on Fundamental Research on Creep and Shrinkage of Concrete (Lausanne, Sept. 1980), Martinus Nijhoff Publishers, The Hague, 1982, pp. 75-92.

13. Reinhardt, H. W.; Pat, M. G. M.; and Wittmann, F. H., "Variability of Creep and Shrinkage of Concrete," *Proceedings,* International Symposium on Fundamental Research on Creep and Shrinkage of Concrete (Lausanne, Sept. 1980), Martinus Nijhoff Publishers, The Hague, 1982, pp. 95-108.

14. Cornelissen, H., "Creep of Concrete—A Stochastic Quantity," PhD thesis, Technical University, Eindhoven, 1979. (in Dutch, with extended English summary)

15. Cornelissen, H., "Creep of Concrete—A Stochastic Quantity," *Proceedings,* International Symposium on Fundamental Research on Creep and Shrinkage of Concrete (Lausanne, Sept. 1980), Martinus Nijhoff Publishers, The Hague, 1982, pp. 109-124.

16. Wittmann, F. H.; Alou, F.; and Ferrari, C., "Experimental Study to Determine Shrinkage and Creep of Concrete," *Report,* Department of Materials, Swiss Federal Institute of Technology, Lausanne, 1985, 18 pp.

17. Wittmann, F. H., "Creep and Shrinkage Mechanisms," *Creep and Shrinkage in Concrete Structures,* Z. P. Bažant and F. H. Wittmann, Editors, John Wiley & Sons, Chichester, 1982, pp. 129-161.

18. Bažant, Z. P., "Mathematical Models for Creep and Shrinkage of Concrete," *Creep and Shrinkage in Concrete Structures,* Z. P. Bažant and F. H. Wittmann, Editors, John Wiley & Sons, Chichester, 1982, pp. 163-256.

19. Madsen, Henrik O., and Bažant, Zdeněk P., "Uncertainty Analysis of Creep and Shrinkage Effects in Concrete Structures," ACI JOURNAL, *Proceedings* V. 80, No. 2, Mar.-Apr. 1983, pp. 116-127.

20. McKay, M. D., "A Method of Analysis of Computer Codes," *Report,* Los Alamos National Laboratory, 1980.

21. McKay, M. D.; Beckman, R. J.; and Conover, W. J., "A Comparison of Three Methods for Selecting Values of Input Variables in the Analysis of Output from a Computer Code," *Technometrics,* V. 21, No. 2, May 1979, pp. 239-245.

22. McKay, M. D.; Conover, W. J.; and Wittmann, D. C., "Report on the Application of Statistical Techniques to the Analysis of Computer Code," *Report* No. LA-NUREG-6526-MS, NRC-4, Los Alamos Scientific Laboratory, 1976.

23. Bažant, Zdeněk, and Liu, Kwang-Liang, "Random Creep and Shrinkage in Structures: Sampling," *Journal of Structural Engineering,* ASCE, V. 111, No. 5, May 1985, pp. 1113-1134.

APPENDIX I — Some consequences of diffusion theory

Let us calculate from nonlinear diffusion theory the initial shape of the shrinkage curve. At the beginning of drying, the drying front moves from the surface into the specimen. For short times, the penetration depth of the drying front δ is small compared to the curvature radius of the surface R which means that initially the drying can be treated as a penetration of the drying front from the surface into a halfspace. The pore relative humidity is initially uniform, $h = h_0$, and it is assumed that at the time t_0 the pore humidity at the surface drops instantly by $\Delta h = h_e - h_0$ where h_e = environmental relative humidity. Neglecting self-desiccation due to hydration and the effect of aging (hydration), the diffusion equation in one dimension may be written as

$$\frac{\partial h}{\partial t} = k \frac{\partial}{\partial x}\left(c \frac{\partial h}{\partial x}\right) \tag{12}$$

in which x = depth coordinate (distance from the surface), c = permeability, and k = slope of the desorption isotherm. Coefficients c and k are functions of pore humidity h.

We now assume the pore humidity distributions at various times to be given as

$$\Delta h = f(\xi), \qquad \xi = x/\delta(t) \tag{13}$$

in which $f(\xi)$ is a certain function giving the shape of the humidity profile, and $\delta(t)$ is a drying penetration depth at time t such that $h = h_0$ for $x > \delta(t)$. The flux of water from the halfspace surface may be expressed as

$$J = -\frac{d}{dt}\int_0^{\delta(t)} F(\Delta h)dx = -\frac{d}{dt}\int_0^1 F[f(\xi)]\, d\xi\, \delta(t) = -c_2\, \dot{\delta}(t) \tag{14}$$

in which $F(\Delta h)$ is the specific water content of concrete (kg per m^3); function $F(\Delta h)$ defines the desorption isotherm. Assuming the humidity profile shapes $f(\xi)$ to be the same for all times, the last integral in Eq. (14) is a constant, denoted as c_2. The flux of water from the surface may be also expressed as

$$\begin{aligned} J &= -c[\text{grad } h]_{x=0} = -c[\partial(\Delta h)/\partial x]_{x=0} = -cf'(0)/\delta(t) \\ &= -c_1/\delta(t) \end{aligned} \tag{15}$$

in which $c_1 = cf'(0)$ = constant if the humidity profile shape remains constant. Equating our two expressions for J, we have $2\dot{\delta}\delta = c_0$ in which $c_0 = 2c_1/c_2$ = constant. This is a differential equation for δ, the solution of which is

$$\delta(t) = [c_0(t-t_0)]^{1/2} \tag{16}$$

It remains to check that the humidity profile indeed keeps the same shape, as assumed. To this end, we substitute Eq. (13) into Eq. (12), which after rearrangements and substitution $\dot{\delta}\delta = c_0/2$ yields the differential equation

$$2k \frac{\partial}{\partial \xi}\left[c \frac{\partial}{\partial \xi} f(\xi)\right] + c_0 \xi \frac{\partial f(\xi)}{\partial \xi} = 0 \tag{17}$$

The coefficients of this differential equation are time-independent, as is the boundary condition. Hence the solution $f(\xi)$ is time-independent, which proves our assumption.

We know that, as a rather good approximation at the beginning, the shrinkage strain may be considered proportional to the total water loss W from the specimen. Thus, we may calculate

$$\epsilon_{sh} = k_s W = k_s \int_0^{\delta(t)} F(\Delta h)dx = k_s \delta(t) \int_0^1 F[f(\xi)]d\xi = k_s k_1 \delta(t) \tag{18}$$

in which the last integral is a constant, denoted as k_1. Now, substituting Eq. (16), we finally obtain for the initial period of drying

$$\epsilon_{sh} = [k_0(t-t_0)]^{1/2} \tag{19}$$

in which $k_0 = c_0 k_s^2 k_1^2$ = constant. This proves that the initial shape of the plot of log ϵ_{sh} versus log $(t-t_0)$ should be a straight line of slope ½, as is verified by the present tests. This property has been known for the linear diffusion theory, however, for concrete it is important that this property also holds for nonlinear diffusion theory.

APPENDIX II — Some other shrinkage formulas

Aside from Eq. (1), other simple formulas exist which exhibit the square-root type time-dependence [Eq. (4)] at early times

$$\epsilon_{sh} = \epsilon_{sh\infty}\left(1 - e^{-(\hat{t}/\tau_{sh})^{1/2r}}\right)^r \tag{20}$$

$$\epsilon_{sh} = \epsilon_{sh\infty}\left[\tanh\left(\frac{\hat{t}}{\tau_{sh}}\right)^r\right]^{1/r} \tag{21}$$

$$\epsilon_{sh} = \epsilon_{sh\infty}\left[\frac{2}{\pi}\arctan\left(\frac{\hat{t}}{\tau_{sh}}\right)^r\right]^{1/r} \tag{22}$$

These formulas, however, differ from Eq. (1) in the long-time asymptotic behavior. For $\hat{t} \to \infty$, Eq. (1), (20), (21) and (22) asymptotically approach the formulas

$$\text{for Eq. (1):} \quad \frac{\epsilon}{\epsilon_{sh\infty}} = 1 - \frac{1}{2r}\left(\frac{\epsilon_{sh}}{t}\right)^r \tag{23}$$

$$\text{for Eq. (20):} \quad \frac{\epsilon}{\epsilon_{sh\infty}} = 1 - re^{-(\hat{t}/\tau_{sh})^{1/2r}} \tag{24}$$

$$\text{for Eq. (21):} \quad \frac{\epsilon}{\epsilon_{sh\infty}} = 1 - \frac{1}{r}e^{-2(\hat{t}/\tau_{sh})^r} \tag{25}$$

$$\text{for Eq. (22):} \quad \frac{\epsilon}{\epsilon_{sh\infty}} = 1 - \frac{1}{\pi r}\left(\frac{\tau_{sh}}{t}\right)^r \tag{26}$$

Now, which asymptotic behavior is more realistic? According to the linear diffusion theory, i.e., for constant diffusivity, the total water loss W from the specimen approaches the final state like a decaying exponential. This happens to be true for Eq. (24) and (25) for $r = 1$. However, in reality the diffusion equation for water in concrete is nonlinear, with the diffusivity strongly decreasing at a decreasing humidity. Therefore, the approach to the final state should be slower than that of a decaying exponential, which means that the function $(1 - \epsilon_{sh}/\epsilon_{sh\infty})/e^{-\hat{t}}$ should be an increasing function of time; this is the case for the inverse (decaying) power functions in Eq. (23) and (26). For Eq. (24) and (25) the approach to the final state seems to be too fast. Consequently, among Eq. (1), (20), (21) and (22), a more realistic asymptotic behavior seems to be exhibited by Eq. (1) and Eq. (22). It should be pointed out, however, that contrary to the initial shrinkage the long-time asymptotic behavior cannot be checked by experimental findings at this moment.

All the formulas in Eq. (20), (21), and (22) have been tried, but none offered any better representation of the present data than Eq. (1) used in the BP model. Numerous other formulas for shrinkage have been proposed in the past, but we need not elaborate on them because their initial behavior contradicts the diffusion theory.